

Dear Prof. Krishnan,

We would like to thank you and the reviewers for the efforts and helpful comments.

We were happy to see that the reviewers found the manuscript important and interesting. As suggested by the reviewers we added more information about previous studies and we added one more plot and text that better quantify the link between SST gradients, surface wind divergence and cloud properties.

Please see the detailed answers to all the reviewers' comments below.

Best wishes,

Ilan Koren

Reply to the two reviewers

We would like to thank the reviewers for their efforts and comments that helped us improve the paper and make it clearer. We have addressed below the two reviewers' comments point by point (the answers are in blue with text cited from the revised manuscript appears in *italics*).

Reviewer # 1:

General comments:

This is very interesting study in understanding the linkage between SWD and properties of the over lying clouds and could be useful in improving the climate modeling capabilities. I think it would be to strengthen the quantification aspect in this research paper as compare with the qualitative description.

Answer: We thank the reviewer for the warm words. We were glad to see that the reviewer likes the paper and thinks it is interesting and beneficial to climate modeling. We have added to the revised manuscript quantification aspects, both in the description of previous works and in our analysis' results regarding the link between surface wind divergence, SST and cloud properties. Please see detailed answers below.

Minor comments:

1. The past studies have presented the quantitative estimates e.g. Cold tongue, warmer ITCZ, increase in the mass flux related to acceleration of the trade winds, the authors may like to consider the same for this study.

Answer: Thank you for this comment. Past studies showed the effect of SST on trade winds that cross the cold tongue towards the ITCZ. Together with the increase in SST the sea surface heat fluxes increase, the vertical mixing increases and the atmospheric boundary layer deepens. As a result they showed that the downward flux of momentum from above increases, the surface winds accelerate and create the surface wind divergence over the SST gradient. Several observational studies presented and quantified these changes in heat fluxes across the equatorial cold tongue-ITCZ complex [Small *et al.*, 2005; Thum *et al.*, 2002; Zhang and McPhaden, 1995]. They estimated a change in sensible heat flux of 6.5-7.5 W m⁻², and a change of 25-35 W m⁻² in latent heat flux both for a 1°C change in SST. We insert these quantitative estimations into the revised introduction section.

Page 1560, the revised text following line 11:

*“Moving northward from the equatorial cold tongue, the atmospheric conditions change gradually. Aircraft measurements at 30 m height in the eastern equatorial Pacific (along 95°W) showed nearly zero latent and sensible heat fluxes over the cold tongue waters (~18°C) and maximal heat fluxes of 160 W m⁻² and 30 W m⁻², respectively, over the warmer waters (~24°C) around 2°N [deSzoeke *et al.*, 2005]. Additional observational studies for the same geographical region [Zhang and McPhaden, 1995; Thum *et al.*,*

2002; Small et al., 2005] estimated changes in fluxes in the range of $6.5\text{-}7.5\text{ W m}^{-2}$ in sensible heat flux and $25\text{-}35\text{ W m}^{-2}$ in latent heat flux both for 1°C change in SST. Over the same region, observations of the marine boundary layer (MBL) depth based on a radiosonde transect along 2°N showed vertical displacement of the inversion layer base height from 1 km over the cold water of the TIW (126°W) to 1.5 km over the warm water (123°W) [Xie, 2004].”

2. Authors may like to illustrate the robustness of the correlation in bringing out the linkage between SWD and cloud properties.

Following this comment we have added the revised paper a new analysis that presents the correlation between the SST gradient, SWD and cloud optical thickness in a clear way. The new figure (Fig. 8), that was added at the end of the results section, presents the new results. A quantitative estimation of the link between SWD and cloud optical depth was added into the text.

Page 1565, from line 19:

“The boreal summer seasons with cold SST, sharp gradSST and strong SWD were characterized by optically thinner clouds (low COT) and a decrease in cloud cover. On the other hand, the boreal winter and spring seasons were characterized by warm SST, mild gradSST, negative SWD and therefore optically thicker clouds (high COT) with larger cloud cover. The evolution of the Atlantic cold tongue and the SWD belt is illustrated by a decrease in SST, increase in gradSST and a sharp transition to minima in COT and CF.

The links between gradSST to SWD and the associated cloud optical thickness were further examined during the boreal summer months. Daily data (in 1° degree) were used for the period of JJA 2007, for the area between $0^\circ\text{-}3^\circ\text{N}$ and $30^\circ\text{W}\text{-}10^\circ\text{W}$ (to ensure large enough dataset). Clear positive correlations are shown between gradSST ($R^2=0.75$) and SWD and inverse correlations with COT. We estimated that in this case and resolution, COT decreased by $\sim 0.57 \pm 0.1$ for increase of $1 \times 10^{-5}\text{ s}^{-1}$ in SWD.”

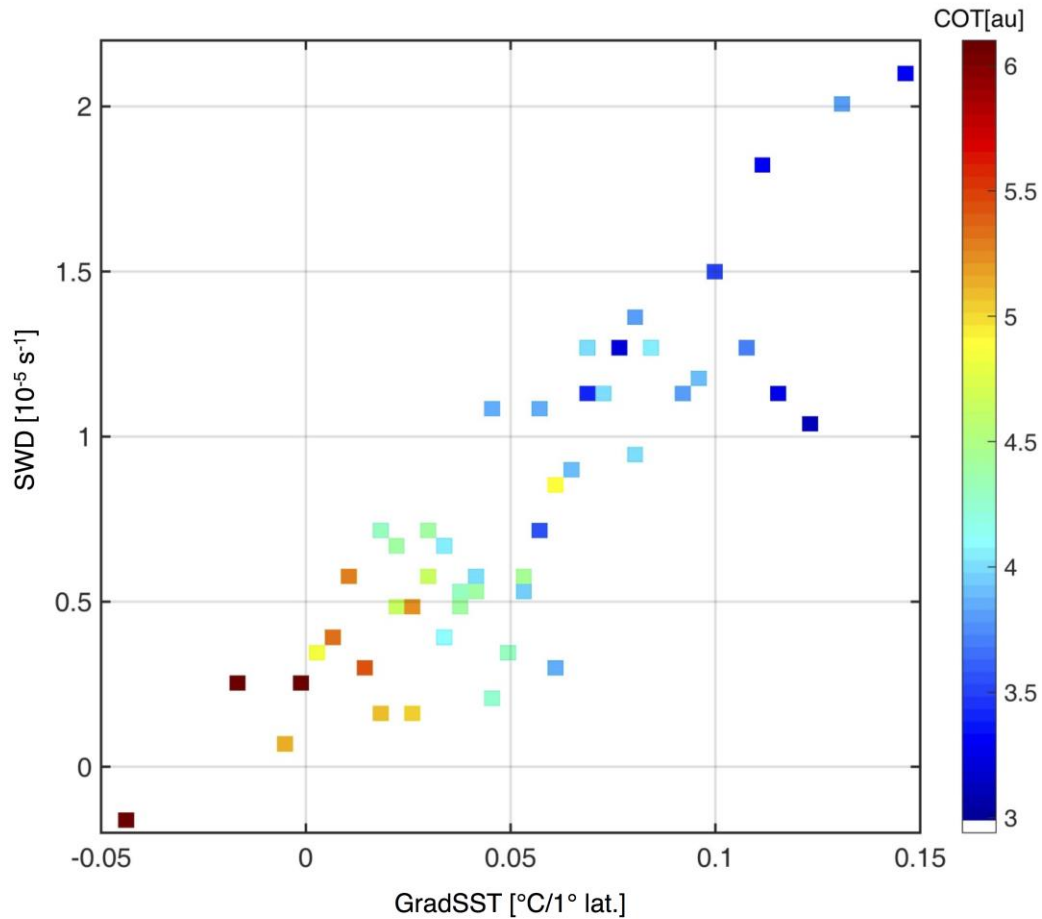


Figure 8. Three-dimensional scatter plot displays the link between daily values of GradSST [°C/1° lat.], SWD [10⁻⁵S⁻¹] and COT [au] over the SWD belt (Latitudes/ Longitudes: 0°-3°N/30°W-10°W), during June, July, and August 2007. Data is divided into 50 equal samples bins.

3. Figure 3a: The legends on X and Y – axes are missing.

Thank you for this comment. Please see below figure 3a with legends on the axes. The information about latitudes and longitudes clarifies the region of interest as presented in the figure.

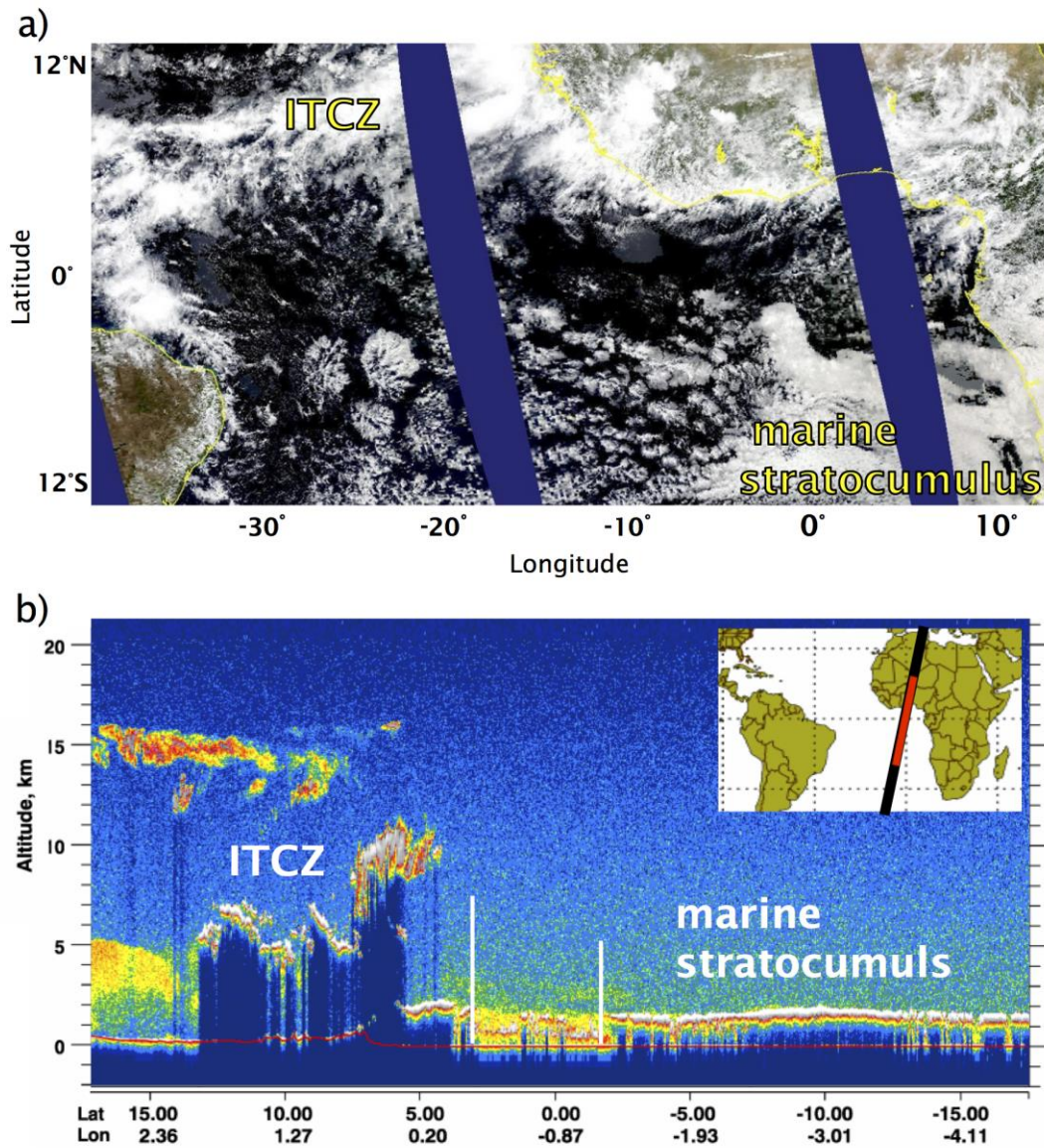


Figure 3. (a) Aqua MODIS true color image (RGB) of the tropical and southern hemisphere subtropical Atlantic Ocean on 8 July 2012. (b) CALIPSO CALIOP 532 nm total attenuation backscatter presenting a vertical profile of cloud and aerosol while crossing the eastern Atlantic Ocean on the same day. Note the area of relatively less cloud amount between the tropical deep convective clouds and subtropical marine stratocumulus decks.

Reviewer # 2:

General comments:

The authors describe a region of significant surface wind divergence between the warm and cool SST region in the equatorial Atlantic that has implications to distinct cloud properties during the boreal summer months, which should be considered as a separate entity for understanding the cloud processes and associated transitions. The findings from the observations are interesting and very well linked to the recent hypotheses proposed by various other researchers. As low level cloud representations in climate models are still intricate, the findings from this study will certainly shed light for improvements. However, there are a few grammar revisions, but minor, that can be taken care of before publication.

Answer: We thank the reviewer for the kind words. We are glad that the reviewer found the paper interesting, well linked to previous studies and helpful for future improvements in climate models. The manuscript was revised according to all the comments. Please see detailed answers below.

Minor comments:

1. Abstract: Refer "southern Hadley cell" as the "southern branch of the Hadley cell in the Atlantic" - this way is referred in many places and it will be good if mentioned with better clarity for the readers.

Answer: Thank you for this comment. We changed the manuscript accordingly.

Page 1558, lines 3-6: *"This belt separates the deep convective clouds of the intertropical convergence zone (ITCZ) from the shallow marine stratocumulus cloud decks forming over the cold-water subtropical region of the southern branch of the Hadley cell in the Atlantic."*

Other places in the manuscript were changed similarly:

Page 1561, lines 14-16: *“Here we argue that when examining meridional features of the southern branch of the marine Hadley cell, the special zone discussed here, located between the cold tongue and the ITCZ, should be considered a unique zone with special wind and cloud patterns.”*

2. "Our findings...." rephrase as "The findings will help to understand the link...."

Answer: Rephrased as suggested.

Page 1558, lines 14-17: *"The findings will help to understand the link between ocean-atmosphere dynamics and cloud properties over this region, and suggest that the SWD zone be considered a unique cloud belt of the southern branch of the Atlantic Hadley cell."*

3. Introduction: Line 66: Remove: "and dictates the location"

Answer: Changed as suggested.

Page 1558, lines 23-25: *“The ITCZ marks the warmest sea surface temperatures (SST) where the Hadley cells converge.”*

4. Line 69: Remove: "apparently mostly" and rephrase it as "seen"

Answer: Rephrased as suggested.

Page 1558, line 26 – Page 1559, line 3: *"As a part of this band there is an area with a zonal belt of surface wind divergence (SWD) that is seen during the boreal summer months [...]"*

5. Line 72: Remove: "suggest" - Rephrase it as "propose"

Answer: Changed as suggested.

Page 1559, lines 4-5: *“In this study, we propose that this oceanic region be considered a unique cloud belt in the southern branch of the Atlantic Hadley cell.”*

6. Line 73: Again mention it as "southern branch of the Atlantic Hadley cell" or you can abbreviate it.

Answer: Changed as suggested.

Page 1559, lines 4-5: *“In this study, we propose that this oceanic region be considered a unique cloud belt in the southern branch of the Atlantic Hadley cell.”*

7. Line 79: Remove "reviewed", just add "e.g."

Answer: Changed as suggested.

Page 1559, lines 8-10: *“Studies on the coupling between SST and the magnitude of surface winds clearly show a positive correlation on spatial scales of 25 to 1,000 km [e.g., Small et al., 2008; Chelton and Xie, 2010].”*

8. Line 125: it should be "during the early boreal summer months"

Answer: Changed as suggested.

Page 1560, lines 1-3: *“These waves form in response to intensification of the southeasterly trade winds and the onset of the equatorial cold tongue during the early boreal summer months.”*

9. Line 131: Replace "have shown this coupling" by "corroborate this coupling from satellite observations"

Answer: Thank you for this comment. We revised the text accordingly.

Page 1560, lines 8-10: *"More recent works corroborate this coupling from satellite observations of SST and high-resolution scatterometer measurements of surface winds in the Pacific and Atlantic cold tongues [...]"*

10. Line 150: Replace "cloudless" by "cloud-free".

Answer: Changed as suggested.

Page 1560, lines 24-27: *"In agreement, Mansbach and Norris [2007] described a decrease in the amount of low-level clouds over the Pacific cold tongue when it is well defined, highlighting the frequent formation of cloud-free boundary layers over the cold tongue."*

11. Lines 151-153: How about the turbulence mechanisms associated with the low-level cloud sustenance? you may need to add this ingredient too.

Answer: Thank you for this comment. We have added to text the contribution of turbulence mixing in the cloud layer.

Page 1561, lines 1-4: *"Under conditions of cold SST and low inversion, inversion-topped marine stratocumulus clouds will form in a structure of closed cells and be maintained by downdrafts driven by cloud-top radiative cooling [Wood, 2012] and turbulent mixing in the cloud layer [Bretherton and Wyant, 1997]."*

12. Line 194: This is not vorticity equation per say. Remove the mention of it.

Answer: We thank the reviewer for this comment. Indeed this is not the vorticity equation. We changed the text to:

Page 1561, lines 25-26: *“The SWD was defined using the divergence term (Eq. 1):*
 $SWD = \partial u/\partial x + \partial v/\partial y$ (1)”

13. Line 223: Strong convergence "not only" dominates.... Please remove the color specifications from the text, it is very clear in the figures.

Answer: Changed as suggested.

Page 1562, line 26 – Page 1563, line 1: *“Strong convergence dominates over the ITCZ belt north of latitude 5°N ($< -1.5 \times 10^{-5} \text{ s}^{-1}$) but also in the area south of the equator, induced by the warm-to-cold SST gradient.”*

14. Line 254: It should be "This is when high values of SWD appeared...."

Answer: Changed as suggested.

Page 1563, lines 25 – 28: *“This is when high values of SWD ($> 1.5 \times 10^{-5} \text{ s}^{-1}$) appeared (while the ITCZ moved northward, May–July), suggesting a link to the sharpest meridional gradient in the SST that forms during this period.”*

15. Line 258: It should be "meridional extent" and not "meridional cover"

Answer: Changed as suggested.

Page 1563, lines 28-29: *“Later, when the ITCZ migrated back toward the equator, the SWD belt was still evident but in a weaker form ($\sim 0.5 \times 10^{-5} \text{ s}^{-1}$) and with smaller meridional extent.”*

16. Line 262: Rephrase as "Clear correlations are evident between..."

Answer: Rephrased as suggested.

Page 1564, lines 3-4: "*Clear correlations are evident between the temporal and spatial variability of the COT and the seasonality and spatial distribution of the SWD belt.*"

17. Line 297: Rephrase as "Zooming in over the SWD region"

Answer: Thank you. Rephrased as suggested.

Page 1564, lines 22-25: "*Zooming in over the SWD region, the link between SST, SST gradient (gradSST) and SWD with time was investigated (Fig. 7), focusing only on the area of the most significant SWD in the central Atlantic (latitudes/longitudes: 0°–2°N/20°W–10°W, green square in Fig. 4a).*"

18. Line 349: Rephrase as "The equatorial Atlantic SWD belt which spans over the central Atlantic between..."

Answer: Changed as suggested.

Page 1566, lines 2-5: "*The equatorial Atlantic SWD belt which spans over the central Atlantic between the equator and 2°N latitude is characterized by a mean monthly divergence higher than $\sim 1.5 \times 10^{-5} \text{ s}^{-1}$ (for a resolution of $1^\circ \times 1^\circ$), which is of the same order of magnitude (but opposite sign) as the average ITCZ convergence.*"

19. Finishing line: Consider a better sentence at the end how this study may help to improve the low-level cloud representation and about the implications of this study in the improvement.

Answer: Thank you for this comment. We modified the last line to:

Page 1567, line 3: “*The appearance of SWD belt during the boreal summer over the Atlantic and the quantitative link between its magnitude and COT as presented here can be used for cloud parameterizations in climate models as well as for model validation for cloud resolving ones.*”

New references that were added into the revised text based on the reviewers

comments:

Small, R. J., Xie, S.-P., Wang, Y., Esbensen, S. K. and Vickers, D.: Numerical Simulation of Boundary Layer Structure and Cross-Equatorial Flow in the Eastern Pacific, J. Atmos. Sci., 62(6), 1812–1830, doi:10.1175/JAS3433.1, 2005.*

Thum, N., Esbensen, S., Chelton, D. B. and McPhaden, M. J.: Air-sea heat exchange along the northern sea surface temperature front in the eastern tropical Pacific, J. Clim., 15(23), 3361–3378, doi:Doi 10.1175/1520-0442(2002)015<3361:Asheat>2.0.Co;2, 2002.

Zhang, G. J. and McPhaden, M. J.: The Relationship between Sea Surface Temperature and Latent Heat Flux in the Equatorial Pacific, J. Clim., 8(3), 589–605, doi:10.1175/1520-0442(1995)008<0589:TRBSST>2.0.CO;2, 1995.

1 **The tropical Atlantic surface wind divergence belt and**
2 **its effect on clouds**

3

4

5

6 **Y. Tubul¹, I. Koren¹, O. Altaratz¹**

7

8 [1] Department of Earth and Planetary Sciences, Weizmann Institute of Science,
9 Rehovot, Israel

10

11 Correspondence to: Ilan.Koren@weizmann.ac.il

12

13

14

15

16

17

18

19

20

21

22

23

24

25

26

27

28

29

30 **Abstract**

31

32 A well-defined surface wind divergence (SWD) belt with distinct cloud properties forms
33 over the equatorial Atlantic during the boreal summer months. This belt separates the
34 deep convective clouds of the intertropical convergence zone (ITCZ) from the shallow
35 marine stratocumulus cloud decks forming over the cold-water subtropical region of the
36 southern branch of the Hadley cell in the Atlantic. Using the QuikSCAT-SeaWinds and
37 Aqua-MODIS instruments, we examined the large-scale spatiotemporal variability of the
38 SWD belt during a 6-year period (2003–2008) and the related links to cloud properties
39 over the Atlantic Ocean. The Atlantic SWD belt was found to be most pronounced from
40 May to August, between the equator and 2°N latitude. A positive correlation and a strong
41 link were observed between formation of the SWD belt and a sharp sea-surface
42 temperature gradient on the northern border of the cold tongue, supporting Wallace’s
43 vertical-mixing mechanism. The dominant cloud type over this region was shallow
44 cumulus. Cloud properties were shown to be strongly linked to the formation and strength
45 of the SWD zone. ~~Our~~The findings will help to understand the link between ocean-
46 atmosphere dynamics and cloud properties over this region, and suggest that the SWD
47 zone be considered a unique cloud belt of the southern branch of the Atlantic Hadley cell.

48

49

50

51

52

53

54

55

56

57

58

59

60 1. Introduction

61

62 The intertropical convergence zone (ITCZ) is located north of the equator throughout the
63 year over the eastern tropical Pacific and Atlantic oceans [Hu *et al.*, 2007]. This defines
64 an interesting narrow belt bounded by the geographical equator and the ITCZ. Both
65 oceanic and atmospheric processes along the geographical equator are affected by
66 changes in the magnitude and sign of the Coriolis force. The ITCZ marks the warmest sea
67 surface temperatures (SST) ~~and dictates the location~~ where the Hadley cells converge.
68 The narrow band between the equator and the ITCZ is therefore controlled by a unique
69 set of oceanic and atmospheric features. As a part of this band there is an area with a
70 zonal belt of surface wind divergence (SWD) that is ~~apparent mostly seen~~
71 boreal summer months (JJA, [Hastenrath and Lamb, 1978; Risien and Chelton, 2008;
72 Zhang *et al.*, 2009]). The SWD strongly affects the properties of clouds that form over
73 and near it. In this study, we ~~suggest propose~~ that this oceanic region be considered a
74 unique cloud belt in the southern branch of the Atlantic Hadley cell.

75

76 Specifically, this narrow belt is bounded by the oceanic cold tongue that forms over the
77 equator during the boreal summer months [Mitchell and Wallace, 1992] and the warmer
78 ITCZ waters (see Fig. 1a). Studies on the coupling between SST and the magnitude of
79 surface winds clearly show a positive correlation on spatial scales of 25 to 1,000 km
80 (~~e.g., reviewed in~~ Small *et al.*, 2008; Chelton and Xie, 2010). The trade winds accelerate
81 as they blow over the SST gradient from cold to warm water. Such acceleration implies
82 an increase in the mass flux out along the wind trajectory that drives local SWD and
83 therefore subsidence of the air mass from above (Fig. 1b). This belt of wind divergence is
84 located (on average) between latitudes 0° and 2°N.

85

86 Two main scenarios have been suggested to explain the link between SST, surface wind
87 speed, and the formation of SWD, the first by Lindzen and Nigam [1987] and the second
88 by Wallace *et al.* [1989]. While both hypotheses explain how the change in SST affects
89 the surface winds to form SWD, each of these mechanisms suggests a different location
90 for the SWD. The first hypothesis suggests that the SWD should overlap the cold SST

91 (i.e. cold tongue) and the second hypothesis links it to the cold-to-warm SST gradient.
92 Figure 2 presents the mean monthly SST for July 2007 in the equatorial Atlantic Ocean
93 (black contours) and the mean SWD field (color). In agreement with *Wallace et al.*'s
94 [1989] theory, anomalous positive values of mean SWD (red color) in July are positioned
95 over the sharp SST gradient on the northern border of the Atlantic cold tongue (Fig. 2a).
96 Moreover, when the equatorial cold tongue and the sharp SST gradient are absent (in
97 October, for example), the SWD belt does not appear (Fig. 2b).

98

99 Previous studies have indicated that the northern and southern borders of the cold tongue
100 are characterized by a pattern of westward-propagating waves termed tropical instability
101 waves (TIW). This is observed in both the Atlantic [*Düing et al.*, 1975] and Pacific
102 [*Legeckis*, 1977] oceans. These waves form in response to intensification of the
103 southeasterly trade winds and the onset of the equatorial cold tongue ~~in~~ during the early
104 boreal summer months. *Hayes et al.* [1989] tested *Wallace et al.*'s [1989] hypothesis and
105 explored how the variability of SST in the eastern Pacific TIW influences the surface
106 winds. They showed high correlations between the meridional SST gradient and the wind
107 speed gradient along the same direction. They also showed that the northern border of the
108 cold tongue is the region with the sharpest SST gradient and the strongest SWD. More
109 recent works corroborate this coupling from ~~have shown this coupling by~~ satellite
110 observations of SST and high-resolution scatterometer measurements of surface winds in
111 the Pacific and Atlantic cold tongues [*Xie et al.*, 1998; *Chelton et al.*, 2001; *Hashizume et*
112 *al.*, 2001].

113

114 Moving northward from the equatorial cold tongue, the atmospheric conditions change
115 gradually. Aircraft measurements at 30 m height in the eastern equatorial Pacific (along
116 95°W) showed nearly zero latent and sensible heat fluxes over the cold tongue waters
117 (~18°C) and maximal heat fluxes of 160 W m⁻² and 30 W m⁻², respectively, over the
118 warmer waters (~24°C) around 2°N [*deSzoeke et al.*, 2005]. Additional observational
119 studies for the same geographical region [*Zhang and McPhaden*, 1995; *Thum et al.*, 2002;
120 *Small et al.*, 2005] estimated changes in fluxes in the range of 6.5-7.5 W m⁻² in sensible
121 heat flux and 25-35 W m⁻² in latent heat flux both for 1°C change in SST. Over the same

122 region, observations of the marine boundary layer (MBL) depth based on a radiosonde
123 transect along 2°N showed vertical displacement of the inversion layer base height from
124 1 km over the cold water of the TIW (126°W) to 1.5 km over the warm water (123°W)
125 [Xie, 2004]. Increased water vapor content over warm water, as well as increased cloud
126 liquid water content and rain amount were observed in an 8-year study over the Atlantic
127 TIW [Wu and Bowman, 2007]. The deepening of the atmospheric MBL and the increase
128 in heat and water vapor fluxes moving from the cold tongue to warmer water favors the
129 formation of marine stratocumulus clouds, as observed from satellite images [Deser et
130 al., 1993]. In agreement, Mansbach and Norris [2007] described a decrease in the
131 amount of low-level clouds over the Pacific cold tongue when it is well defined,
132 highlighting the frequent formation of cloud-freeless boundary layers over the cold
133 tongue.

134

135 The strength of the inversion layer and SST have been shown to be main players in
136 determining the atmospheric conditions, and hence cloud properties, over the subtropical
137 oceans [Albrecht et al., 1995; Myers and Norris, 2013]. Under conditions of cold SST
138 and low inversion, inversion-topped marine stratocumulus clouds will form in a structure
139 of closed cells and be maintained by downdrafts driven by cloud-top radiative cooling
140 [Wood, 2012] and turbulent mixing in the cloud layer [Bretherton and Wyant, 1997]. This
141 gradually transforms into an open cell structure and then to trade cumulus clouds while
142 moving to regions with warmer water (dictating larger fluxes) and the MBL inversion
143 climbs and becomes weaker [Wyant et al., 1997]. Such transitions are valid as one moves
144 westward or southward (toward the equator) from the eastern shores of the subtropical
145 oceans off Africa or America, with upwelling-driven cold SSTs, experiencing gradual
146 warming of the SST and deepening of the MBL. This transition is characterized by a
147 distinct decrease in cloud cover with a minimum over the trade cumulus regime
148 [Muhlbauer et al., 2014]. Figure 3 shows the ITCZ and shallow Marine Stratocumulus
149 (MSc) clouds regimes characterized by high cloud cover and the decrease in cloud cover
150 between them.

151

152 | Here we argue that when examining meridional features of the southern branch of the
153 | marine Hadley cell, the special zone discussed here, located between the cold tongue and
154 | the ITCZ, should be considered a unique zone with special wind and cloud patterns.

155 |
156 |

157 | **2. Data and Methods**

158 |

159 | Observational data retrieved from high-resolution active and passive satellite instruments
160 | were used to specify the equatorial SWD belt, cold tongue, and cloud properties.
161 | Analyses were based on a full 6 years of daily data collected from 2003 to 2008.

162 | The SWD was calculated using $0.25^\circ \times 0.25^\circ$ resolution surface wind measurements from
163 | the SeaWinds active microwave scatterometer instrument on board the QuikSCAT
164 | (Quick Scatterometer) satellite. Launched in 1999 [Spencer *et al.*, 2000], SeaWinds
165 | passes twice a day (06:30 and 18:30 local time), measuring surface wind speed and
166 | direction at 10 m above sea level. The SWD was defined using a divergence term
167 | vorticity equation (Eq. 1):

$$168 | \text{SWD} = \partial u / \partial x + \partial v / \partial y \quad (1)$$

169 | where u and v are the zonal and meridional components of the wind. Wind divergence is
170 | presented in units of m s^{-1} per distance of 1° degree (~ 100 km), which is equal to 10^{-5} s^{-1} .
171 | The monthly mean divergence ranged mostly between 2 and $-2 \times 10^{-5} \text{ s}^{-1}$, where negative
172 | divergence is referred to as convergence. Examining the ITCZ through the SWD showed
173 | that it is characterized by mean values of around $-1.5 \times 10^{-5} \text{ s}^{-1}$ during most of the year
174 | (Fig. 4). QuikSCAT provides surface wind data under both clear and cloudy conditions,
175 | but possible errors can be caused by rain [Draper and Long, 2004]. The monthly mean
176 | SWD values used here were calculated using daily data.

177 | SST [Esaias *et al.*, 1998] and cloud properties [cloud optical thickness (COT), and cloud
178 | fraction (CF), Platnick *et al.*, 2003] were obtained from the moderate resolution imaging
179 | spectroradiometer (MODIS) instrument on board the Aqua satellite (equatorial crossing
180 | at 01:30 and 13:30 local time).

181 Our research domain was set to cover the equatorial Atlantic cold tongue and the SWD
182 belt. Therefore, an area between 10°N and 10°S is presented in the first part of the results
183 section. The focused investigation of the SWD belt was performed over a subset of this
184 area located in the central Atlantic (20°W–10°W), between 0° and 2°N latitude, covering
185 the belt of maximum mean SWD (Fig. 4a).

186

187

188 3. Results

189

190 The spatial association between SST, SWD and cloud properties (COT and CF) was
191 examined first. Figure 4 presents maps of mean monthly SWD, cloud properties (colors)
192 and SST (black contours) for July 2007. The SWD belt (colored in red) is evident (Fig.
193 4a) along the sharp SST gradient at the northern border of the equatorial cold tongue.
194 Note that the TIW cannot be recognized in a monthly average SST field due to the same
195 (monthly) characterization time scale of this phenomenon. High SWD values ($>1.5 \times 10^{-5}$
196 s^{-1}) can be recognized slightly south of the equator over the eastern Atlantic, and between
197 | latitudes 0° and 2°N over the central Atlantic. Strong convergence-~~(blue color)~~ dominates
198 over the ITCZ belt north of latitude 5°N ($<-1.5 \times 10^{-5} s^{-1}$) but also in the area south of the
199 equator, induced by the warm-to-cold SST gradient. Two fundamental properties of
200 clouds are presented as well, the COT (Fig. 4b) and daytime CF (Fig. 4c).

201

202 The deep convective clouds over the ITCZ (COT > 10), but also in the western
203 subtropical Atlantic (COT > 7, colored in turquoise–yellow) were characterized by high
204 COT. As the eastern subtropical SST gets warmer toward the west or toward the ITCZ,
205 the MBL becomes deeper, permitting formation of thicker low clouds ($5 < \text{COT} < 10$). A
206 cloudy area characterized by relatively low COT (<5) formed between the subtropical
207 and ITCZ belts, with the lowest values centered along the sharp SST gradient (the SWD
208 belt).

209

210 The map of CF spatial distribution (Fig. 4c) presents high values over the deep
211 convective ITCZ belt (with SST > 27°C) and over the subtropical eastern Atlantic (with

212 SST < 24°C), whereas over the belt between them, the cloud cover was significantly
213 smaller. Specifically, the lowest CF values (<0.4) were between latitudes 5°S and 0°,
214 overlapping the cold tongue area.

215

216 We examined the annual variability of the SWD belt and cloud properties in the central
217 Atlantic between longitudes 20°W and 10°W (defined by the yellow square in Fig. 4a).
218 Figure 5 presents Hovmöller diagrams for the years 2003 to 2008. The upper panel (Fig.
219 5a) shows the changes along the years in the position and magnitude of the SWD. In this
220 domain (i.e. the central Atlantic), the SWD forms around May–June and remains until
221 August–September. It is prominent between the equator and 2°N latitude. The patterns of
222 the SWD belt correlate with the migration of the ITCZ belt in the northern hemisphere
223 (as illustrated by the blue color in Fig. 5a). The ITCZ belt is positioned closer to the
224 equator during the months of December to April, and in May, it migrates northward,
225 reaching its most poleward northern position during July–August. This is when Hhigh
226 values of SWD ($>1.5 \times 10^{-5} \text{ s}^{-1}$) appeared (while the ITCZ moved northward, (May–July),
227 suggesting a link to the sharpest meridional gradient in the SST that forms during this
228 period. Later, when the ITCZ migrated back toward the equator, the SWD belt was still
229 evident but in a weaker form ($\sim 0.5 \times 10^{-5} \text{ s}^{-1}$) and with smaller meridional ~~extente~~over.
230 The SWD was not evident between December and April when the ITCZ was in its closest
231 position to the equator.

232 ~~We saw e~~Clear correlations are evident between the temporal and spatial variability of
233 the COT and the seasonality and spatial distribution of the SWD belt. A clear minimum
234 in COT (<5) was seen in the area between the equator and 2°N from May to August (Fig.
235 5b). The CF's temporal evolution was similar, but with a slight southward shift in the
236 location of the minimum synclines toward the cold tongue (Fig. 5c). To quantify the
237 strength and robustness of the correlations, we extracted the central part around our study
238 area (between latitudes 3°N and 6°S) of the COT and CF Hovmöller matrixes and
239 checked the correlations for a gradual shift between each of them and the SWD matrix.
240 The 2D correlation was calculated for each displacement between the two matrixes (Fig.
241 6). Both COT and CF matrixes showed that the peak in correlations with the SWD
242 corresponds to no shift in time. The peak correlation with COT was $R = 0.74$, showing a

243 perfect match with the SWD (no shift in latitude or time). The peak correlation with CF
244 was $R = 0.75$, corresponding to a shift of 2° southward relative to the SWD field, and
245 suggesting a stronger link to the cold SST south of the equator. Note the oscillations
246 along the time axis indicating a peak in the correlations when the shift matches 1 year. A
247 secondary maximum is shown when the latitudinal shift is large enough to correlate with
248 the marine stratocumulus decks in the south. A minimum is shown when the latitudinal
249 shift to the north is large enough to correlate over the opposite trends of the ITCZ.

250 Zooming in ~~over~~ the SWD region, the link between SST, meridional SST-gradient of
251 SST (gradSST) and SWD with time was investigated (Fig. 7), focusing only on the area
252 of the most significant SWD in the central Atlantic (~~longitudes~~/latitudes/longitudes: 0° –
253 2°N / 20°W – 10°W / ~~0° – 2°N~~ , green square in Fig. 4a). Monthly mean SST (Fig. 7a) ranged
254 between $\sim 29^\circ\text{C}$ around March–May to $\sim 24^\circ\text{C}$ around July–August. The changes in SST
255 with time showed a relatively rapid cooling period compared to the warming period, in
256 agreement with the known dynamics of the equatorial Atlantic cold tongue [Okumura
257 and Xie, 2004]. The sharpest SST gradients (Fig. 7b) appeared about a month before the
258 mean SST minimum (i.e. June or July). Here, positive values of gradSST reflected SST
259 warming from the equator northward. Temporal variability of SWD (Fig. 7c) behaved
260 like a combination of the SST and meridional gradSST fields. It had rapid evolving and
261 slow decaying times, similar to the SST field, but its maximal values clearly correlated in
262 time with the gradSST peaks (June or July, marked by red-shaded columns).

263
264 The most pronounced SWD belt appeared (June/July depending on the year, Fig. 7)
265 before the beginning of the coldest SST phase (July/August). This trend could be related
266 to the northward migration of the ITCZ. During the stage at which the equatorial cold
267 tongue begins to evolve, the ITCZ location is relatively closer to the equator and
268 therefore, the ratio between the temperature differences and distance from the equator
269 northward (i.e. gradSST) is the largest. When the cold tongue is well established and the
270 ITCZ is in a northern-most position (July/August), both gradSST and SWD are on their
271 descending branch. When the ITCZ is close to the equator (December–March), the

272 equatorial SST is warm, gradSST is at its minimal values and the SWD exhibits its
273 minimal (negative) values (i.e., convergence).

274

275 The mean COT over the location of the prominent SWD belt (between 0° and 2°N
276 latitudes) varied between 2 and 13 (Fig. 7d), and the mean CF over this region ranged
277 between 0.4 and 0.9 (Fig. 7e). Both cloud characteristics showed a distinct seasonal link
278 to the activity of ocean-atmosphere dynamic features. The boreal summer seasons with
279 cold SST, sharp gradSST and strong SWD were characterized by optically thinner clouds
280 (low COT) and a decrease in cloud cover. On the other hand, the boreal winter and spring
281 seasons were characterized by warm SST, mild gradSST, negative SWD and therefore
282 optically thicker clouds (high COT) with larger cloud cover. The evolution of the Atlantic
283 cold tongue and the SWD belt is illustrated by a decrease in SST, increase in gradSST
284 and a sharp transition to minima in COT and CF.

285 The links between gradSST to SWD and the associated cloud optical thickness were
286 further examined during the boreal summer months. Daily data (in 1° degree) were used
287 for the period of JJA 2007, for the area between 0°–3°N and 30°W–10°W (to ensure
288 large enough dataset). Clear positive correlations are shown between gradSST ($R^2=0.75$)
289 and SWD and inverse correlations with COT. We estimated that in this case and
290 resolution, COT decreased by $\sim 0.57 \pm 0.1$ for increase of $1 \times 10^{-5} \text{ s}^{-1}$ in SWD.

291

292

293 **4. Summary and Discussion**

294

295 The equatorial Atlantic SWD belt which spans over the central Atlantic between the
296 equator and 2°N latitude and is characterized by a mean monthly divergence higher than
297 $\sim 1.5 \times 10^{-5} \text{ s}^{-1}$ (for a resolution of 1° x 1°), which is of the same order of magnitude (but
298 opposite sign) as the average ITCZ convergence. It is most pronounced from May to
299 August. Here we show a positive correlation and tight connection in space and time
300 between the (large-scale) distribution of sharp mean monthly gradSST and SWD. These
301 results support vertical mixing as the responsible mechanism [Wallace *et al.* 1989] for
302 formation of the SWD belt over the northern SST front of the Atlantic cold tongue.

303

304 Investigating the link of cloud properties to the SWD and cold tongue, we show that the
305 COT correlates in space and time with gradSST and SWD, whereas CF correlates better
306 with SST. We show that the minimum COT is located exactly over the sharp SST
307 gradient and the SWD belt (0° – 2° N), while the area of minimum cloud cover overlaps the
308 cold tongue (5° S– 1° N). Temporal analysis focusing on the SWD belt only showed
309 similar results (Fig. 7). Shallow cumulus clouds, which are the dominant clouds in the
310 SWD region, form under moderate SST conditions ($\sim 24^{\circ}$ C– 27° C) and their coverage was
311 positively correlated with SST. The cumulus cloud COT and CF were highly correlated
312 with the magnitude of the SWD (Fig. 7).

313

314 Previous studies have shown a gradual decrease in cloud cover along the subtropical-to-
315 tropical cloud transition [*Sandu et al.*, 2010; *Muhlbauer et al.*, 2014], with a minimum
316 over the trade cumulus region. But in general, this transition has received little attention
317 in observational studies and climate models find it difficult to correctly represent its
318 properties. The subtropical-to-tropical cloud transition was recently investigated in the
319 Northeastern Pacific Ocean to provide a framework for evaluating climate-model results
320 against observations [*Karlsson et al.*, 2010; *Teixeira et al.*, 2011]. Over the Atlantic
321 Ocean, the belt bounded by the equator (in the south) and the ITCZ is better defined, and
322 therefore the SWD and its links to cloud properties are clearer. Our results suggest that
323 this belt should be considered a separate entity of the southern branch of the Hadley cell
324 over the Atlantic. A better understanding of the essential dynamic features and their link
325 to cloud properties over this narrow strip may help improve low-level cloud
326 representation in climate models. The appearance of SWD belt during the boreal summer
327 over the Atlantic and the quantitative link between its magnitude and COT as presented
328 here can be used for cloud parameterizations in climate models as well as for model
329 validation for cloud resolving ones.

330

331

332

333 **Acknowledgements**

334 The research leading to these results received funding from the European Research
335 Council under the European Union's Seventh Framework Programme (FP7/2007-
336 2013)/ERC Grant agreement no. 306965.

337

338 **References**

- 339 Albrecht, B. a., Bretherton, C. S., Johnson, D., Scubert, W. H. and Frisch, a. S.: The
340 Atlantic Stratocumulus Transition Experiment—ASTEX, *Bull. Am. Meteorol. Soc.*,
341 76(6), 889–904, doi:10.1175/1520-0477(1995)076<0889:TASTE>2.0.CO;2, 1995.
- 342 Chelton, D. and Xie, S.: Coupled Ocean-Atmosphere Interaction at Oceanic Mesoscales,
343 *Oceanography*, 23(4), 52–69, doi:10.5670/oceanog.2010.05, 2010.
- 344 Chelton, D. B., Esbensen, S. K., Schlax, M. G., Thum, N., Freilich, M. H., Wentz, F. J.,
345 Gentemann, C. L., McPhaden, M. J. and Schopf, P. S.: Observations of Coupling
346 between Surface Wind Stress and Sea Surface Temperature in the Eastern Tropical
347 Pacific, *J. Clim.*, 14(7), 1479–1498, doi:10.1175/1520-
348 0442(2001)014<1479:OOCBSW>2.0.CO;2, 2001.
- 349 Deser, C., Wahl, S. and Bates, J.: The influence of Sea surface temperature gradients on
350 stratiform cloudiness along the equatorial front in the Pacific ocean, *J. Clim.*, 6(6), 1172 –
351 1180, doi:10.1175/1520-0442(1993)006<1172:TIOSST>2.0.CO;2, 1993.
- 352 deSzoeko, S. P., Bretherton, C. S., Bond, N. A., Cronin, M. F. and Morley, B. M.: EPIC
353 95W Observations of the Eastern Pacific atmospheric boundary layer from the cold
354 tongue to the ITCZ, *J. Atmos. Sci.*, 62(2), 426–442, doi:10.1175/JAS-3381.1, 2005.
- 355 Draper, D. W. and Long, D. G.: Evaluating the effect of rain on SeaWinds scatterometer
356 measurements, *J. Geophys. Res.*, 109(C02005), doi:10.1029/2002JC001741, 2004.
- 357 Düing, W., Hisard, P., Katz, E., Meincke, J., Miller, L., Moroshkin, K. V., Philander, G.,
358 Ribnikov, A. A., Voigt, K. and Weisberg, R.: Meanders and long waves in the equatorial
359 Atlantic, *Nature*, 257, 280 – 284, doi:doi:10.1038/257280a0, 1975.
- 360 Esaias, W. E., Abbott, M. R., Barton, I., Brown, O. B., Campbell, J. W., Carder, K. L.,
361 Clark, D. K., Evans, R. H., Hoge, F. E., Gordon, H. R., Balch, W. M., Letelier, R. and

362 Minnett, P. J.: An overview of MODIS capabilities for ocean science observations, IEEE
363 Trans. Geosci. Remote Sens., 36(4), 1250–1265, doi:10.1109/36.701076, 1998.

364 Hashizume, H., Xie, S.-P., Liu, W. T. and Takeuchi, K.: Local and remote atmospheric
365 response to tropical instability waves: A global view from space, J. Geophys. Res.,
366 106(D10), 10,173–10,185, doi:10.1029/2000JD900684, 2001.

367 Hastenrath, S. and Lamb, P.: On the dynamics and climatology of surface flow over the
368 Equatorial oceans, Tellus A, 30(1978), 436–448, doi:10.3402/tellusa.v30i5.10387, 1978.

369 Hayes, S. P., McPhaden, M. J. and Wallace, J. M.: The Influence of Sea-Surface
370 Temperature on Surface Wind in the Eastern Equatorial Pacific: Weekly to Monthly
371 Variability, J. Clim., 2(12), 1500–1506, doi:10.1175/1520-
372 0442(1989)002<1500:TIOSST>2.0.CO;2, 1989.

373 Hu, Y., Li, D. and Liu, J.: Abrupt seasonal variation of the ITCZ and the Hadley
374 circulation, Geophys. Res. Lett., 34(18), L18814, doi:10.1029/2007GL030950, 2007.

375 Karlsson, J., Svensson, G., Cardoso, S., Teixeira, J. and Paradise, S.: Subtropical Cloud-
376 Regime Transitions: Boundary Layer Depth and Cloud-Top Height Evolution in Models
377 and Observations, J. Appl. Meteorol. Climatol., 49(9), 1845–1858,
378 doi:10.1175/2010JAMC2338.1, 2010.

379 Legeckis, R.: Long waves in the eastern equatorial pacific ocean: a view from a
380 geostationary satellite., Science, 197(4309), 1179–1181,
381 doi:10.1126/science.197.4309.1179, 1977.

382 Lindzen, R. S. and Nigam, S.: On the role of sea surface temperature gradients in forcing
383 low-level winds and convergence in the tropics, J. Atmos. Sci., 44, 2418–2436,
384 doi:10.1175/1520-0469(1987)044<2418:OTROSS>2.0.CO;2, 1987.

385 Mansbach, D. K. and Norris, J. R.: Low-Level Cloud Variability over the Equatorial Cold
386 Tongue in Observations and Models, J. Clim., 20(8), 1555–1570,
387 doi:10.1175/JCLI4073.1, 2007.

388 Mitchell, T. and Wallace, J.: The annual cycle in equatorial convection and sea surface
389 temperature, J. Clim., 5(10), 1140 – 1156, doi:10.1175/1520-
390 0442(1992)005<1140:TACIEC>2.0.CO;2, 1992.

391 Muhlbauer, a., McCoy, I. L. and Wood, R.: Climatology of stratocumulus cloud
392 morphologies: microphysical properties and radiative effects, *Atmos. Chem. Phys.*
393 *Discuss.*, 14(5), 6981–7023, doi:10.5194/acpd-14-6981-2014, 2014.

394 Myers, T. a. and Norris, J. R.: Observational Evidence That Enhanced Subsidence
395 Reduces Subtropical Marine Boundary Layer Cloudiness, *J. Clim.*, 26(19), 7507–7524,
396 doi:10.1175/JCLI-D-12-00736.1, 2013.

397 Okumura, Y. and Xie, S. P.: Interaction of the Atlantic equatorial cold tongue and the
398 African monsoon, *J. Clim.*, 17, 3589–3602, doi:10.1175/1520-
399 0442(2004)017<3589:IOTAEC>2.0.CO;2, 2004.

400 Platnick, S., King, M. D., Ackerman, S. A., Menzel, W. P., Baum, B. A., Riédi, J. C. and
401 Frey, R. A.: The MODIS cloud products: Algorithms and examples from Terra, *Geosci.*
402 *Remote Sensing, IEEE Trans.*, 41(2), 459–473, doi:10.1109/TGRS.2002.808301, 2003.

403 Risien, C. M. and Chelton, D. B.: A Global Climatology of Surface Wind and Wind
404 Stress Fields from Eight Years of QuikSCAT Scatterometer Data, *J. Phys. Oceanogr.*,
405 38(11), 2379–2413, doi:10.1175/2008JPO3881.1, 2008.

406 Sandu, I., Stevens, B., Pincus, R. and Angeles, L.: On the transitions in marine boundary
407 layer cloudiness, *Atmos. Chem. Phys.*, 2377–2391, doi:10.5194/acpd-9-23589-2009,
408 2010.

409 Small, R. J., deSzoeke, S. P., Xie, S. P., O’Neill, L., Seo, H., Song, Q., Cornillon, P.,
410 Spall, M. and Minobe, S.: Air–sea interaction over ocean fronts and eddies, *Dyn. Atmos.*
411 *Ocean.*, 45(3-4), 274–319, doi:10.1016/j.dynatmoce.2008.01.001, 2008.

412 [Small, R. J., Xie, S.-P., Wang, Y., Esbensen, S. K. and Vickers, D.: Numerical](#)
413 [Simulation of Boundary Layer Structure and Cross-Equatorial Flow in the Eastern](#)
414 [Pacific*, *J. Atmos. Sci.*, 62\(6\), 1812–1830, doi:10.1175/JAS3433.1, 2005.](#)

415 Spencer, M. W., Wu, C., Long, D. G. and Member, S.: Improved Resolution Backscatter
416 Measurements with the SeaWinds Pencil-Beam Scatterometer, *IEEE Trans. Geosci.*
417 *Remote Sens.*, 38(1), 89–104, doi:10.1109/36.823904, 2000.

418 Teixeira, J., Cardoso, S., Bonazzola, M., Cole, J., DelGenio, a., DeMott, C., Franklin, C.,
419 Hannay, C., Jakob, C., Jiao, Y., Karlsson, J., Kitagawa, H., Köhler, M., Kuwano-

420 Yoshida, a., LeDrian, C., Li, J., Lock, a., Miller, M. J., Marquet, P., Martins, J., Mechoso,
421 C. R., Meijgaard, E. V., Meinke, I., Miranda, P. M. a., Mironov, D., Neggers, R., Pan, H.
422 L., Randall, D. a., Rasch, P. J., Rockel, B., Rossow, W. B., Ritter, B., Siebesma, a. P.,
423 Soares, P. M. M., Turk, F. J., Vaillancourt, P. a., Von Engeln, a. and Zhao, M.: Tropical
424 and Subtropical Cloud Transitions in Weather and Climate Prediction Models: The
425 GCSS/WGNE Pacific Cross-Section Intercomparison (GPCI), *J. Clim.*, 24(20), 5223–
426 5256, doi:10.1175/2011JCLI3672.1, 2011.

427 | [Thum, N., Esbensen, S., Chelton, D. B. and McPhaden, M. J.: Air-sea heat exchange](#)
428 [along the northern sea surface temperature front in the eastern tropical Pacific, *J. Clim.*,](#)
429 [15\(23\), 3361–3378, doi:Doi 10.1175/1520-0442\(2002\)015<3361:Asheat>2.0.Co;2, 2002.](#)

430 Wallace, J. M., Mitchell, T. P. and Deser, C.: The Influence of Sea-Surface Temperature
431 on Surface Wind in the Eastern Equatorial Pacific: Seasonal and Interannual Variability,
432 *J. Clim.*, 2(12), 1492–1499, doi:10.1175/1520-0442(1989)002<1492:TIOSST>2.0.CO;2,
433 1989.

434 Wood, R.: Stratocumulus Clouds, *Mon. Weather Rev.*, 140(8), 2373–2423,
435 doi:10.1175/MWR-D-11-00121.1, 2012.

436 Wu, Q. and Bowman, K. P.: Multiyear satellite observations of the atmospheric response
437 to Atlantic tropical instability waves, *J. Geophys. Res.*, 112(D19104),
438 doi:10.1029/2007JD008627, 2007.

439 Wyant, M. C., Bretherton, C. S., Rand, H. a. and Stevens, D. E.: Numerical Simulations
440 and a Conceptual Model of the Stratocumulus to Trade Cumulus Transition, *J. Atmos.*
441 *Sci.*, 54(1), 168–192, doi:10.1175/1520-0469(1997)054<0168:NSAACM>2.0.CO;2,
442 1997.

443 | Xie, S., Ishiwatari, M., Hashizume, H. and Takeuchi, K.: Coupled ocean-atmospheric
444 waves on the equatorial front, *Geophys. Res. Lett.*, 25(20), 3863,
445 doi:10.1029/1998GL900014, 1998.

446 Xie, S. P.: Satellite observations of cool ocean-atmosphere interaction, *Bull. Am.*
447 *Meteorol. Soc.*, 85(2), 195–208, doi:10.1175/BAMS-85-2-195, 2004.

448 [Zhang, G. J. and McPhaden, M. J.: The Relationship between Sea Surface Temperature](#)
449 [and Latent Heat Flux in the Equatorial Pacific, J. Clim., 8\(3\), 589–605,](#)
450 [doi:10.1175/1520-0442\(1995\)008<0589:TRBSST>2.0.CO;2, 1995.](#)

451 Zhang, Y., Stevens, B., Medeiros, B. and Ghil, M.: Low-Cloud Fraction, Lower-
452 Tropospheric Stability, and Large-Scale Divergence, J. Clim., 22(18), 4827–4844,
453 doi:10.1175/2009JCLI2891.1, 2009.

454

455

456

457 **Figure 1.** (a) A schematic map of the main tropical Atlantic players from May to August.
458 (b) A north–south cross section along the narrow band between the equatorial cold
459 tongue and the intertropical convergence zone (ITCZ) showing acceleration of the trade
460 wind path along the sharp sea-surface temperature (SST) gradient which imposes surface
461 wind divergence.

462

463 **Figure 2.** Tropical Atlantic monthly maps of mean surface wind divergence [in units of
464 10^{-5} s^{-1} , color] and sea surface temperature [$^{\circ}\text{C}$, black contours] for (a) July and (b)
465 October, 2007, using QuikSCAT-SeaWinds and MODIS-Aqua.

466

467 **Figure 3.** (a) Aqua MODIS true color image (RGB) of the tropical and southern
468 hemisphere subtropical Atlantic Ocean on 8 July 2012. (b) CALIPSO CALIOP 532 nm
469 total attenuation backscatter presenting a vertical profile of cloud and aerosol while
470 crossing the eastern Atlantic Ocean on the same day. Note the area of relatively less
471 cloud amount between the tropical deep convective clouds and subtropical marine
472 stratocumulus decks.

473

474 **Figure 4.** Monthly-mean maps of (a) surface wind divergence (in units of 10^{-5} s^{-1}), (b)
475 cloud optical thickness (in arbitrary units), and (c) daytime cloud cover fraction
476 (normalized units between 0 and 1) during July 2007. SST [$^{\circ}\text{C}$] is presented as black

477 contours in all panels. The yellow and green boxes in Fig. 4a define the areas focused on
478 in Figs. 5 and 6.

479

480 **Figure 5.** Latitude–time Hovmöller diagrams (2003–2008) of zonal and monthly mean
481 (a) surface wind divergence [10^{-5} s^{-1}], (b) cloud optical thickness, and (c) cloud fraction.
482 The central Atlantic section (20°W – 10°W) averaged for these Hovmöller diagrams is in
483 the yellow square in Figure 4a.

484

485 **Figure 6.** Correlation matrixes between the Hovmöller diagrams of the surface wind
486 divergence (SWD, with a negative sign) and the cloud optical thickness (COT, left) and
487 the cloud fraction (CF, right). Both matrixes show that the correlation peaks correspond
488 to no shift in time (X axis). The peak correlation with COT, $R = 0.74$, also corresponds to
489 no shift in latitude (Y axis). The peak correlation with CF, $R = 0.75$, corresponds to a 2°
490 southward shift relative to the SWD field, suggesting a stronger link to the cold SST over
491 the equator than to meridional SST-gradient of SST (gradSST).

492

493 **Figure 7.** Mean monthly time series (2003–2008) of oceanic and atmospheric dynamic
494 state and cloud properties along the equatorial Atlantic (Latitudes/Longitudes:- 0° – 2°N
495 / 20°W – 10°W , ~~Lat. 0° – 2°N~~). The presented fields are (a) sea-surface temperature (SST),
496 (b) meridional gradient of SST, (c) surface wind divergence (SWD), (d) total cloud
497 optical thickness (COT), and (e) daytime cloud cover fraction (CF, in normalized units
498 between 0 and 1).

499

500 **Figure 8.** Three-dimensional scatter plot displays the link between daily values of
501 GradSST [$^{\circ}\text{C}/1^{\circ} \text{ lat.}$], SWD [10^{-5} s^{-1}] and COT [au] over the SWD belt
502 (Latitudes/Longitudes: 0° – $3^{\circ}\text{N}/30^{\circ}\text{W}$ – 10°W), during June, July, and August 2007. This
503 plot illustrates the robustness of the correlations between the three parameters using a
504 daily resolution. The relevant data is divided into 50 bins that contain equal number of
505 samples.

506

507